Physical Science International Journal

Volume 28, Issue 6, Page 1-20, 2024; Article no.PSIJ.123693
ISSN: 2348-0130

Modeling Heat and Mass Transfer in a Wet Terracotta Tube Channel for Evaporative Cooling Application: Influence of Geometrical Parameters

ZOUNGRANA Windnigda [a,b*], BOUKAR Makinta [a], COULIBALY Ousmane [b], TUBREOUMYA Guy Christian [b] and BERE Antoine [b]

[a] West African Science Service Center on Climate Change and Adapted Land Use, Graduate Research Program on Climate Change and Energy (GRP-CCE), Laboratoire d'Energétique, d'Electronique, d'Electrotechnique, d'Automatique et d'informatique Industrielle (LAERT-LA2EI), University ABDOU MOUMOUNI, Niamey, Niger.
[b] Laboratoire de Physique et de Chimie de l'Environnement, l'Université Joseph KI ZERBO, Ouagadougou, Burkina Faso.

Authors' contributions

This work was carried out in collaboration among all authors. Author ZW conceived the ideas and the experimental designed of the study, performed experiments/data collection, performed the data analysis and interpretation, and wrote the first draft of the manuscript. Author BM and Author CO contributed to the methodology and provided revisions to scientific content of the manuscript. Author TGC and Author BA provide access to crucial research materials. All authors read and approved the final manuscript.

Article Information

DOI: https://doi.org/10.9734/psij/2024/v28i6855

Open Peer Review History:
This journal follows the Advanced Open Peer Review policy. Identity of the Reviewers, Editor(s) and additional Reviewers, peer review comments, different versions of the manuscript, comments of the editors, etc are available here: https://www.sdiarticle5.com/review-history/123693

Original Research Article

Received: 20/07/2024
Accepted: 24/09/2024
Published: 28/09/2024

**Corresponding author: E-mail: windnigda@gmail.com;*

Cite as: *Windnigda, ZOUNGRANA, BOUKAR Makinta, COULIBALY Ousmane, TUBREOUMYA Guy Christian, and BERE Antoine. 2024. "Modeling Heat and Mass Transfer in a Wet Terracotta Tube Channel for Evaporative Cooling Application: Influence of Geometrical Parameters". Physical Science International Journal 28 (6):1-20. https://doi.org/10.9734/psij/2024/v28i6855.*

ABSTRACT

This study investigates the influence of design parameters on the performance of a terracotta tube-type evaporative cooling system. A mathematical model was developed based on double film theory and energy and mass conservation equations of the humid air and the wet tube wall in a one-dimensional geometry by applying correlations for heat and mass transfer coefficients and air psychometric properties. A system of non-linear differential equations was established and analytically integrated to obtain the relationship between the operating and the geometrical parameters of the system. Various geometrical parameters were simulated to assess their effects on outlet air temperature, cooling capacity, and wet-bulb effectiveness. The results indicate that increasing the tube equivalent diameter results in higher outlet temperatures and cooling capacity but decreases wet-bulb effectiveness. Conversely, an increased flatness ratio significantly enhances cooling performance and wet-bulb effectiveness due to a larger surface area for heat exchange. Additionally, longer tubes correlate with lower outlet temperatures and higher cooling capacity, indicating improved cooling performance. These findings emphasize the importance of selecting appropriate tube dimensions to optimize cooling efficiency in evaporative cooling systems. By balancing hydraulic diameter, flatness ratio, and tube length, engineers can design compact and effective cooling solutions suitable for various applications, ultimately contributing to energy-efficient and sustainable cooling technologies. The modeling approach developed in this study can also be applied to address challenges in geothermal energy extraction, drying of porous solids, food processing and storage, building thermal insulation, nuclear reactor cooling, and seawater desalination.

Keywords: Mathematical modeling; porous terracotta tube; direct evaporative cooling; tubular heat; mass exchanger.

1. INTRODUCTION

As global temperatures continue to rise and urbanization accelerates, the demand for energy-efficient cooling solutions has never been more critical [1]. Traditional air conditioning systems, while effective, contribute significantly to energy consumption and greenhouse gas emissions [2]. In regions with hot and dry climates, space cooling accounts for over 50% of total building energy use [3]. Developing energy-efficient air-conditioning technologies is essential for reducing this consumption. Evaporative cooling (EC), which uses the latent heat from water evaporation to cool air, is a promising alternative to traditional vapor compression systems due to their energy efficiency and environmental sustainability [4]. EC systems primarily consume energy through pumps and fans, indicating potential for significant energy savings [5]. The wet media is an essential component in an EC system [6].

Terracotta, a porous ceramic material, has garnered attention for its potential in evaporative cooling applications due to its unique properties. The material's thermal mass and porosity can enhance heat and mass transfer processes, making it an attractive choice for evaporative cooling systems. Due to its high porosity, low density, large specific surface area, and high thermal conductivity [7], porous ceramic enhances EC performance in several ways. Firstly, its porosity and capillary action improve surface hydrophilicity, enhancing wettability. Secondly, its large specific surface area increases the contact between the working air and the water film. Thirdly, the porous structure acts as a water reservoir, allowing for intermittent rather than continuous water spraying, which reduces the energy consumption of the circulating pump [8]. Among the various shapes of porous ceramic media, hollow clay tubes arranged to form a bundle also gain popularity as an evaporative cooling medium. Early research in porous ceramic tubular evaporative cooling focuses on cross-flow semi-indirect configurations [9,10]. Except for Semi-IEC, the integration of porous ceramic tubes with heat pipes (HP) for indirect evaporative cooling systems has also been extensively investigated. The use of porous ceramic tubes allows for effective heat and mass transfer, while heat pipes can provide efficient heat recovery for sensible cooling applications. For instance, Amer and Boukhanouf [11] conducted an experimental investigation to evaluate the effect of various operation conditions on a novel heat pipe and ceramic tube-based evaporative cooler. Their cooler was able to drop the inlet air temperature

by 12℃, and a wet bulb effectiveness of 86% was achievable. More recently, Rajski et al. [12] developed a mathematical model to investigate the performance of gravity-assisted heat pipe-based indirect evaporative cooler (GAHP-based IEC). They state that the proposed cooler can be used as a complementary device to conventional HVAC systems. By modeling the heat and mass transfer dynamics within wet terracotta tube channels, researchers can elucidate the influence of various geometrical parameters, such as tube diameter, length, and flatness ratio, on the overall cooling performance.

Several studies have explored the impact of tube geometry on evaporative cooling efficiency. Adam et al. [13] performed analysis of indirect evaporative cooler performance under various heat and mass exchanger dimensions and flow parameters and found that the optimal dimensions that give good efficiency in climates with moderate humidity, the length of the duct should be between 0.6 to 1.0 m, the width of the channel between 0.3 to 0.5 m, and the channel gap between 0.004 to 0.008 m. Similarly, Sun et al. [14] reported that increasing the equivalent diameter of porous ceramic pipes in an indirect evaporative cooler resulted in lower outlet temperatures and higher wet-bulb effectiveness. Sulaiman and Adham [15] developed a numerical model to investigate four new geometries of heat and mass exchanger for dew point evaporative cooling and their performance is compared to that of the commonly used flat plate and corrugated plate exchangers. The analysis revealed that the circular concentric tube exchanger, under certain operating conditions produced the lowest air temperature and the highest wet bulb and dew point effectiveness while the triangular tube exchanger achieved the highest cooling capacity and coefficient of performance.

Recent research has largely focused on round tubular EC, but flat tubular variants, which offer several advantages, have not been as thoroughly investigated. Unlike round tubular ECs, flat tubular ECs provide superior wetting characteristics, leading to better formation of water films and more efficient use of water's latent heat. Additionally, flat tubular ECs lead to more compact systems rather than round tubular configuration. These advantages have made flat tubular ECs a growing area of interest. Hasan and Sirén [16] provides a comprehensive overview of evaporative cooling systems, highlighting the advantages of flat tubular configurations in terms of surface area and heat exchange efficiency. The increased surface area in flat tubes facilitates better contact between the air and the wetted surface, leading to enhanced evaporative cooling performance, particularly in hot and dry climates. Liu et al. [17] developed a direct-expansion ice thermal storage system that incorporates a multi-channel flat-tubular evaporator, analyzing key factors to enhance system performance. Existing studies have explored the impact of geometric parameters on the cooling performance of Terracotta Tubular ECs (TTEC) through experimental testing and numerical simulations. Despite these advancements, existing studies still lack efficiency and effectiveness in evaluating and predicting TTEC performance. Optimization strategies for this kind of cooler remain underexplored, and there is a pressing need for direct, pragmatic approaches for its performance evaluation. To date, no research has developed performance prediction models for TTEC using analytical methods or engaged in comprehensive multi-objective optimization.

This study focuses on the innovative application of wet terracotta tube channels in evaporative cooling systems, where the unique properties of terracotta such as its thermal mass and porosity can enhance heat and mass transfer processes. By modeling the heat and mass transfer dynamics within these tube channels, we aim to elucidate the influence of various geometrical parameters, including tube diameter, length, and flatness ratio, on the overall cooling performance. Understanding the intricate relationship between these geometrical factors and system efficiency is essential for optimizing the design of terracotta tube-based evaporative coolers. As we delve into the modeling of these systems, we not only seek to advance the scientific understanding of heat and mass transfer in porous materials but also to contribute to the development of more efficient and sustainable cooling technologies. This research holds the potential to inform the design of next-generation evaporative cooling systems that can significantly reduce energy consumption while providing effective climate control in a variety of applications, particularly in hot and arid regions.

2. MATERIALS AND METHODS

2.1 Geometric Parameters of the Tubular Heat and Mass Exchanger

The heat and mass exchanger geometry is shown in Fig. 1.

To characterize the geometry of this type of heat and mass exchanger, three parameters are essential: tube short axis (a), tube long axis (a+b), and tube length (L). The other parameters namely, perimeter (P), cross-section area (A_c), exchange surface area (A_w), tube Flatness Ratio (R_F), and characteristic length (represented by hydraulic diameter (D_H) or equivalent diameter (D_e), are derived using specific formulas.

- **Perimeter:**

$$P=\pi a+2b \quad (1)$$

- **Cross-section area:**

$$A_c = \frac{a^2\pi}{4} + ab \quad (2)$$

- **Wet surface area:**

The wet surface area is computed using eq. (3)

$$Aw=L[\pi a+2b] \quad (3)$$

- **Hydraulic and equivalent diameters:**

Before determining the heat and mass transfer coefficients, it is necessary to establish an appropriate Reynolds number for the flat tube geometry. For air flowing through non-circular tubes, usually, the hydraulic diameter is used for Reynolds number calculations, which is: determining the heat and mass transfer coefficients, it is necessary to establish an appropriate Reynolds number for the flat tube geometry. For air flowing through non-circular tubes, usually, the hydraulic diameter is used for Reynolds number calculations, which is:

$$D_H = \frac{4A_c}{P} \quad (4)$$

However, as mentioned by Cheng et al.by[18], for non-circular channels, using equivalent diameters instead of hydraulic diameters in the flow analysis is recommended. Using the equivalent diameter allows for keeping the same mass flow rate of air in the equivalent tube as that in the flat tube. Hence, in this study, the equivalent diameter is treated as the characteristic diameter for the flat tube. Its expression is given by:

$$D_e = \sqrt{\frac{4A_c}{\pi}} \quad (5)$$

- **Tube Flatness Ratio (FR)**

The tube flatness ratio is defined as the ratio of the tube's long axis and the tube's short axis:

$$R_F = \frac{a+b}{a} \quad (6)$$

When the equivalent diameter and the flatness ratio are known, a and b can be determined by solving the equation below:

$$A_c = \frac{\pi {D_e}^2}{4} = \frac{a^2\pi}{4} + ab \quad (7)$$

For $R_F = 1 \rightarrow b = 0 \; and \; a = D_e \rightarrow$ $this\ correspond\ to\ the\ circular\ tube$

For $R_F = 2 \rightarrow b = a \; and \; a = D_e\sqrt{(\pi/4)/(1+\pi/4))}$

For $R_F = 3 \rightarrow b = 2a \; and \; a = D_e\sqrt{(\pi/4)/(2+\pi/4))}$

For $R_F = 4 \rightarrow b = 3a \; and \; a = D_e\sqrt{(\pi/4)/(3+\pi/4))}$

The geometric dimensions of the tubes are listed in Table 1.

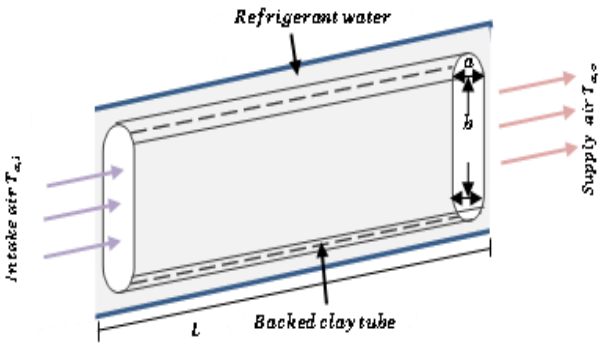

Fig. 1. Baked clay tube heat and mass exchanger geometry

Table 1. Geometric dimensions of the tube

Tube	D_e (mm)	a (mm)	b (mm)	P_w (mm)	A_c (mm^2)	D_h (mm)	R_F
Round	15	15	0	47.12	176.71	15	1
AR2	15	9.95	9.95	51.15	176.71	13.82	2
AR3	15	7.96	15.93	56.88	176.71	12.43	3
AR4	15	6.83	20.50	62.46	176.71	11.32	4

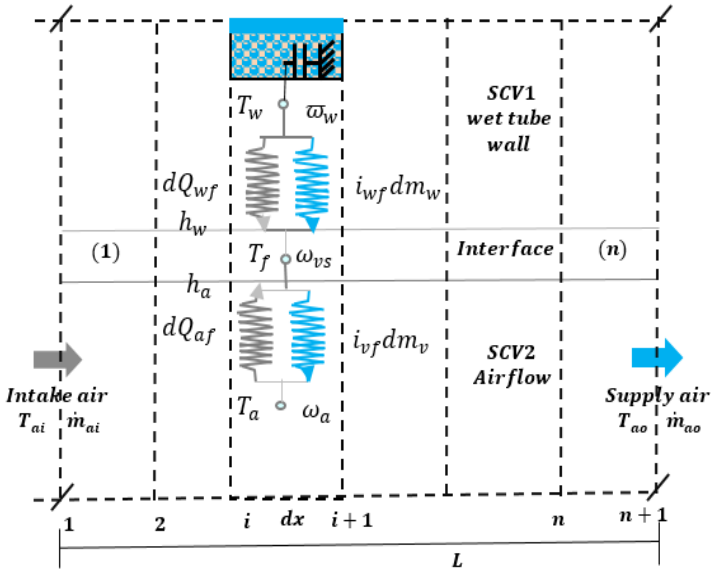

Fig. 2. Physical model of the heat and mass exchanger

Table 1 shows that the equivalent diameter is larger than the hydraulic diameter with increasing differences at higher flatness ratios.

2.2 Description of the Physical Model

The physical description of the tubular heat and mass exchanger involves a control volume where heat and mass conservation laws are applied to analyze the cooling process. The system features a porous tube that allows water to seep through via capillary action, moving toward the inner surface, and evaporates in contact with hot dry air flowing inside the tube, creating a cooling effect at the tube-air interface. The basic heat and mass exchange process diagram is shown in Fig. 2.

2.3 Simplifying Assumptions

In the following analysis, it is assumed that:

- Heat and mass are transferred perpendicularly through the channel walls;
- Within the air streams, the convective heat transfer is considered the dominant mechanism for heat transfer;
- The interior surface of the tube's wall is completely and continuously wet;
- All outside boundaries are adiabatic;
- Tube-air interface temperature is assumed identical to the wet bulb temperature of the intake air;
- Air is treated as an incompressible gas and the velocity and properties of the supply air are considered to be uniform in a differential control volume;
- No condensation happens in the air channel;
- The heat and mass transfer coefficients are constant in a differential control volume.

By employing these assumptions, the mathematical model of the evaporative cooler can now be derived from energy and mass conservation equations.

2.4 Governing Equations

The physical model is divided into numerous control volumes with an infinitesimal wet surface area of $\left|A_w.\frac{dx}{L}\right|$. A set of differential equations is

established for one control volume using the energy and mass conservation laws. Fig. 3 shows an elementary control volume of length dx with three zones: the wet clay tube zone (SCV1), the airflow zone, and the tube-air interface zone (SCV2). The wet clay tubes exchange sensible heat dQ_{wf} and latent heat $i_{wf}dm_w$ with the interface through the tubes' walls. It is also indicated that the interface draws part of its evaporation energy dQ_{af} from the process air. The water vapor produced is then absorbed by the process air as a form of latent heat $i_{vf}d\dot{m}_v$.

Let dm_e be the evaporation rate, ϖ the specific humidity of clay tubes, and ω_a the specific humidity of process air:

$$\varpi_t = \frac{m_w}{m_t} \tag{8}$$

$$\omega_a = \frac{\dot{m}_v}{\dot{m}_a} \tag{9}$$

Considering the heat and mass transfer process at the water-air interface of the evaporative cooling system, the general energy and mass conservation equations are given below:

The mass balance across each control volume is given by:

For the dry air

$$d\dot{m}_a = 0 \tag{10}$$

For the dry tube

$$dm_t = 0 \tag{11}$$

For the liquid water

$$dm_w = m_t d\varpi_t = -dm_e \tag{12}$$

For the water vapor

$$d\dot{m}_v = \dot{m}_a d\omega_a = dm_e \tag{13}$$

The mass balance of the elementary control volume comprising all the fluids is written as:

$$dm_t + dm_w + d\dot{m}_a + d\dot{m}_v = 0 \tag{14}$$

Carrying eqs (10),(11),(12), and (13) into eq. (14), we find:

$$m_t d\varpi_t = -\dot{m}_a d\omega_a \tag{15}$$

If $i_t, i_w, i_a and\ i_v$, are the enthalpies of dry tubes, water, dry air and water vapor respectively, by neglecting heat exchange with the environment and variations in kinetic and potential energies, the energy balance for each sub-control volume is:

$$CV1:\ d(m_t i_t) + d(m_w i_w) = -dQ_{wf} - i_{wf}dm_e \tag{16}$$

$$CV2:\ d(\dot{m}_a i_a) + d(\dot{m}_v i_v) = -dQ_{af} + i_{vf}dm_e \tag{17}$$

Where i_{wf} and i_{vf} are the specific enthalpies of the water and the water vapor evaluated at the wet surface-air interface temperature T_f.

$$i_{wf} = c_{pw}T_f \tag{18}$$

$$i_{vf} = i_0 + c_{pv}T_f \tag{19}$$

Where i_0 is the latent heat of vaporization of water at 0 °C.

The energy balance of the elementary control volume comprising all the fluids is written as:

$$d(m_t i_t) + d(m_w i_w) + d(\dot{m}_a i_a) + d(\dot{m}_v i_v) = 0 \tag{20}$$

Carrying eqs (16)&(17) into eq.(21), we find:

$$dQ_{wf} + dQ_{af} = \left(i_{vf} - i_{wf}\right)dm_e \tag{21}$$

We assume that the water vapor produced at the wet surface-air interface is saturated at water film temperature (T_f), which means that equilibrium between the liquid and vapor phases is established at the interface, so the previous expression takes the form:

$$dQ_{wf} + dQ_{af} = i_{fg}dm_e \tag{22}$$

Where i_{fg} is the latent heat of the vaporization of water at the water film temperature.

Eq.(22) indicates that the net sensible heat flux at the water-air interface represents the energy required for the evaporation process.

$$i_{fg} = i_0 + (c_{pv} - c_{pw})T_f \tag{23}$$

The value of i_{fg} is can be calculated with a relative error of less than 1% by the following formula valid between 0 and 180°C[19]:

$$i_{fg} = 2501.6 - 2.18T_f \ (kJ.kg^{-1}) \quad (24)$$

Where T_f is the water film temperature.

The equations established previously are written in terms of flows of mass and heat, and now these same flow equations will be expressed in terms of transfer potentials.

Vapor density gradients are responsible for mass transfer. The mass flow between the interface and the airstream is defined by the relationship:

$$dm_e = h_m(\rho_{vf} - \rho_v)\frac{A_w}{L}dx \quad (25)$$

Where ρ_v is the partial density of the water vapor in air and ρ_{vf} is the partial density of the saturated water vapor at T_f and is, therefore, a function of T_f: $\rho_{vf} = f(T_f)$ and in which, h_m is the mass transfer coefficient. $\rho_v(T)$ is linked to the specific humidity by eq.(26).

$$\rho_v = \rho_a\omega_a \quad (26)$$

Where ρ_a is the density of the dry air. Since the partial density of water vapor is proportional to the moisture content of the air, the difference between the moisture content of the saturated air at the interface and that of the passing air is the driving force for water evaporation in the wet channel. Then, eq. (25) can be rewritten as follows:

$$dm_e = \rho_a h_m(\omega_{vs} - \omega_a)\frac{A_w}{L}dx \quad (27)$$

Where ω_a is the moisture content of the air (kg/kg_{as}) and ω_{vs} is the moisture content of saturated air close to the wet surface. ω_{vs} is evaluated at water film temperature using eq. (28)[20].

$$\omega_{vs}(T_f) = 0.622\frac{P_{vs}(T_f)}{101325 - P_{vs}(T_f)} \quad (28)$$

In which $P_{vs}(T_f)$ is the saturated vapor pressure calculated at wet surface temperature T_f and whose correlation expression is given by[21].

The mass change for each sub-control volume can be rewritten as follows:

$$\frac{m_t d\varpi_t}{dt} = -\rho_a h_m(\omega_{vs} - \omega_a)\frac{A_w}{L}dx \quad (29)$$

$$\dot{m}_a d\omega_a = \rho_a h_m(\omega_{vs} - \omega_a)\frac{A_w}{L}dx \quad (30)$$

In a similar way to mass transfer, temperature gradients are the potentials that cause heat transfer. The enthalpy change for each sub-control volume can be rewritten as follows:

$$d(m_t i_t) + d(m_w i_w) = m_t di_t + i_t dm_t + i_w dm_w + m_w di_w \quad (31)$$

$$d(\dot{m}_a i_a) + d(\dot{m}_v i_v) = i_a d\dot{m}_a + \dot{m}_a di_a + i_v d\dot{m}_v + \dot{m}_v di_v \quad (32)$$

$$d(m_t i_t) + d(m_w i_w) = m_t(c_{pt} + \varpi_t c_{pw})dT_w + c_{pw}T_w dm_w \quad (33)$$

$$d(\dot{m}_a i_a) + d(\dot{m}_v i_v) = \dot{m}_a(c_{pa} + \omega_a c_{pv})dT_a + (i_0 + c_{pv}T_a)d\dot{m}_v \quad (34)$$

The heat fluxes transferred between subsystem CV2 and the interface, and between subsystem CV1 and the interface, are respectively defined by the relationships:

$$dQ_{wf} = k_w(T_w - T_f)\frac{A_w}{L}dx \quad (35)$$

$$dQ_{af} = h_a(T_a - T_f)\frac{A_w}{L}dx \quad (36)$$

Where h_a is the convective heat transfer coefficient between air and the interface. For the flowing air condition, h_a is a function of air flow rate and channel characteristics. A is the total internal surface area of a tube, and L is the tube length. k_w is the total heat transfer coefficient between the whole system's thermal mass and the interface and is defined as follows:

$$k_w = \frac{1}{\frac{1}{h_{wt}} + \frac{\delta}{\lambda_{wt}}} \quad (37)$$

Where h_{wt} represents the convective heat transfer coefficient between the refrigerant water and the tube's external wall. δ and λ_{wt} represent the thickness and thermal conductivity of wet channel walls respectively. The porous ceramic wall is saturated with water and its thermal conductivity should take into account both the dry ceramic and water thermal conductivities. This is computed as follows:

$$\lambda_{wt} = \frac{\lambda_w[\lambda_w + \lambda_t - (1-\sigma)(\lambda_w - \lambda_t)]}{\lambda_w + \lambda_t + (1-\sigma)(\lambda_w - \lambda_t)} \tag{38}$$

λ_t is the thermal conductivity of the dry ceramic container and σ is the ceramic container's porosity. λ_w is the thermal conductivity of water.

Finally, by substituting the heat and mass flow expressions in eqs (16), (17), and (21) by their corresponding heat and mass transfer expressions, we obtain the following relationship:

$$\frac{m_t(c_{pt} + \varpi_t c_{pw})dT_w}{dt} + k_w(T_w - T_f)\frac{A_w}{L}dx - c_{pw}(T_w - T_f)dm_e = 0 \tag{39}$$

$$\dot{m}_a(c_{pa} + \omega_a c_{pv})dT_a + h_a(T_a - T_f)\frac{A_w}{L}dx + c_{pv}(T_a - T_f)dm_e = 0 \tag{40}$$

$$k_w(T_w - T_f) + h_a(T_a - T_f) = \rho_a h_m i_{fg}(T_f)(\omega_{vs} - \omega_a) \tag{41}$$

The above equations can also be combined into a system of five differential equations as follows:

$$\begin{aligned}\{\frac{d\varpi_t}{dt} &= -\frac{\rho_a h_m A_w dx}{m_t L}(\omega_{vs} - \omega_a) \quad \frac{d\omega_a}{dx} = \frac{A_w \rho_a h_m}{L\dot{m}_a}(\omega_{vs} - \omega_a) \quad \frac{dT_w}{dt} \\ &= \frac{\left[-k_w + c_{pw}\rho_a h_m(\omega_{vs} - \omega_a)\right]A_w dx}{m_t(c_{pt} + \varpi_t c_{pw})L}(T_w - T_f) \quad \frac{dT_a}{dx} \\ &= -\frac{\left[h_a + c_{pv}\rho_a h_m(\omega_{vs} - \omega_a)\right]A_w}{\dot{m}_a(c_{pa} + \omega_a c_{pv})L}(T_a - T_f)\, k_w(T_w - T_f) + h_a(T_a - T_f) \\ &= \rho_a h_m i_{fg}(T_f)(\omega_{vs} - \omega_a)\end{aligned} \tag{42}$$

Analytical model development: This system describes the heat and mass transfer process in the cooler at unsteady-state conditions. Studying such a system would involve solving these equations simultaneously to examine the evolution of the system and the impact of the initial and operating parameters. Unfortunately, it is a system of nonlinear equations that cannot be solved numerically by the finite difference method. Nevertheless, at steady-state conditions, this system is reduced to three main equations that can be combined and integrated to obtain an analytical solution. In the absence of heat extraction from the system thermal mass (water-tube assembly), and without heat addition from any external source, the system becomes adiabatic, open and the process evolves in a steady state for heat and mass transfer. At steady state conditions, the whole thermal mass of the system is in thermal equilibrium with the tube-air interface. In this case, the recirculating water and the interface are at the same temperature, and this temperature is that of the wet bulb temperature of the inlet air. Hence, at a steady state, the energy required to sustain the evaporation is exclusively provided by the convective heat transfer from the air flowing inside the tube channels. Therefore eq. (39) disappears and eq. (41) is simplified to:

$$h_a(T_a - T_{wb}) = \rho_a h_m i_{fg}(T_f)(\omega_{vs} - \omega_a) \tag{43}$$

Therefore, at a steady state, the cooler is described by the following set of equations:

$$\begin{aligned}&\{\frac{d\varpi_t}{dt} = -\frac{\rho_a h_m A_w dx}{m_t L}(\omega_{vs} - \omega_a) \\ &\frac{d\omega_a}{dx} = \frac{A_w \rho_a h_m}{L\dot{m}_a}(\omega_{vs} - \omega_a)\end{aligned} \qquad \frac{dT_a}{dx} = -\frac{[h_a + c_p}{\dot{m}_a} \Big/ h_a(T_a - T_{wb}) \tag{44}$$

Determination of the exchange surface area: Eqs. (43)&(44) are combined and integrated to determine the wet surface area as a function of the inlet and outlet air temperatures, air physical properties, air mass flow rate, and heat and mass transfer coefficients. From eq.(43):

$$\frac{h_a(T_a - T_{wb})}{i_{fg}} = \rho_a h_m(\omega_{vs} - \omega_a) \tag{45}$$

$$\omega_a = \left(\frac{i_{fg}\rho_a h_m \omega_{vs} - h_a(T_a - T_{wb})}{i_{fg}\rho_a h_m}\right) \tag{46}$$

From eq.(44):

$$\frac{dT_a}{dx} = -\frac{[h_a + c_{pv}\rho_a h_m(\omega_{vs} - \omega_a)]A_w}{\dot{m}_a(c_{pa} + \omega_a c_{pv})L}(T_a - T_{wb}) \tag{47}$$

Replacing the specific humidity of air (ω_a) in eq.(40) with its expression in equation (39) gives:

$$\frac{dT_a}{dx} = -\frac{\frac{h_a[i_{fg} + c_{pv}(T_a - T_{wb})]A_w(T_a - T_{wb})}{i_{fg}}}{\dot{m}_a L\left(\frac{i_{fg}\rho_a h_m c_{pa} + c_{pv} i_{fg}\rho_a h_m \omega_{vs} - c_{pv} h_a(T_a - T_{wb})}{i_{fg}\rho_a h_m}\right)} \tag{48}$$

$$\frac{dT_a}{dx} = -\frac{A_w\rho_a h_m h_a[i_{fg} + c_{pv}(T_a - T_{wb})](T_a - T_{wb})}{\dot{m}_a L i_{fg}\rho_a h_m c_{pa} + \dot{m}_a L c_{pv} i_{fg}\rho_a h_m \omega_{vs} - \dot{m}_a L c_{pv} h_a(T_a - T_{wb})} \tag{49}$$

$$\frac{dT_a}{dx} = -\frac{A_w\rho_a h_m h_a i_{fg}(T_a - T_{wb}) + A_w\rho_a h_m h_a c_{pv}(T_a - T_{wb})^2}{\dot{m}_a L i_{fg}\rho_a h_m c_{pa} + \dot{m}_a L c_{pv} i_{fg}\rho_a h_m \omega_{vs} - \dot{m}_a L c_{pv} h_a(T_a - T_{wb})} \tag{50}$$

$$\frac{dT_a[i_{fg}\rho_a h_m(c_{pa} + c_{pv}\omega_{vs}) - c_{pv} h_a(T_a - T_{wb})]}{i_{fg}(T_a - T_{wb}) + c_{pv}(T_a - T_{wb})^2} = -\frac{A_w\rho_a h_m h_a}{\dot{m}_a L}dx \tag{51}$$

By posing:

$$\left\{\begin{array}{lll} y = T_a - T_{wb} & a = i_{fg}\rho_a h_m(c_{pa} + c_{pv}\omega_{vs}) & c = i_{fg} \\ NUT = \frac{A_w\rho_a h_m h_a}{\dot{m}_a L} & b = -c_{pv} h_a & e = c_{pv} \end{array}\right. \tag{52}$$

Eq.(51) can be rewritten as follows:

$$\frac{dy[a + by]}{cy + ey^2} = -NUTdx \tag{53}$$

The simple element decomposition of the function $\frac{a+by}{cy+ey^2}$ gives:

$$\frac{a + by}{cy + ey^2} = \frac{a + by}{y(c + ey)} = \left[\frac{k_1}{y} + \frac{k_2}{c + ey}\right] = \frac{k_1(c + ey) + k_2 y}{y(c + ey)} \tag{54}$$

$$\frac{a + by}{cy + ey^2} = \frac{ck_1 + (k_1 e + k_2)y}{y(c + by)} \tag{55}$$

By identification, the constants k_1 and k_2 are given:

$$\left\{ck_1 = a\ k_1 e + k_2 = b\ \rightarrow \begin{array}{l} k_1 = \frac{a}{c} = \rho_a h_m\left(c_{pa} + c_{pv}\omega_{vs}\right) \\ k_2 = b - \frac{ad}{c} = -c_{pv} h_a - \rho_a h_m(c_{pa} + c_{pv}\omega_{vs})c_{pv} \end{array}\right. \tag{56}$$

Eq. (53) can be rewritten as:

$$\frac{k_1 dy}{y} + \frac{k_2 dy}{c + ey} = -NUTdx \tag{57}$$

Integrating eq.(57) gives:

$$k_1 \int_{y_i}^{y_o} \frac{dy}{y} + \frac{k_2}{e} \int_{y_i}^{y_o} \frac{edy}{c + ey} = -NUT \int_0^L dx \tag{58}$$

$$k_1 \, ln \, ln \, \frac{y_o}{y_i} + \frac{k_2}{e} \, ln \, ln \, \frac{c + ey_o}{c + ey_i} = -NUT \times L \tag{59}$$

By replacing the coefficients and variables with their values, we obtain:

$$\rho_a h_m (c_{pa} + c_{pv}\omega_{vs}) \, ln \, ln \left[\frac{T_{a,o} - T_{wb}}{T_{a,i} - T_{wb}}\right] - (h_a + \rho_a h_m (c_{pa} + c_{pv}\omega_{vs})) \, ln \, ln \left[\frac{i_{fg} + c_{pv}(T_{a,o} - T_{wb})}{i_{fg} + c_{pv}(T_{a,i} - T_{wb})}\right] = -\frac{A_w \rho_a h_m h_a}{\dot{m}_a} \tag{60}$$

$$A_w = \frac{\dot{m}_a}{\rho_a h_m h_a}\left[\left(h_a + \rho_a h_m (c_{pa} + c_{pv}\omega_{vs})\right) ln \, ln \left[\frac{i_{fg} + c_{pv}(T_{a,o} - T_{wb})}{i_{fg} + c_{pv}(T_{a,i} - T_{wb})}\right] - \rho_a h_m (c_{pa} + c_{pv}\omega_{vs}) \, ln \, ln \left[\frac{T_{a,o} - T_{wb}}{T_{a,i} - T_{wb}}\right]\right] \tag{61}$$

Determination of outlet air temperature: If the exchange surface area is known, then we can solve the outlet temperature numerically with computer code. The computer algorithm for this purpose is set as follows:

1. $Start$

2. $Constants\ declaration$

3. $T_{a,o} \leftarrow T_{a,i}$

4. $Error \leftarrow 1$

5. $While\ (Error > 0.0001)$

6. $Error \leftarrow \left| A_w - \frac{\dot{m}_a}{\rho_a h_m h_a}\left[\left(h_a + \rho_a h_m (c_{pa} + c_{pv}\omega_{vs})\right) ln \, ln \left[\frac{i_{fg} + c_{pv}(T_{a,o} - T_{wb})}{i_{fg} + c_{pv}(T_{a,i} - T_{wb})}\right] - \rho_a h_m (c_{pa} + c_{pv}\omega_{vs}) \, ln \, ln \left[\frac{T_{a,o} - T_{wb}}{T_{a,i} - T_{wb}}\right]\right]\right|$

7. $T_{a,o} \leftarrow T_{a,o} - 0.001$

8. $End\ loop$

9. $Display\ T_{a,o}$

10. End

Cooling efficiency: The effectiveness of a DEC system for lowering the inlet airflow temperature is measured by its cooling efficiency defined by [22] as follows:

$$\varepsilon_{wb} = \frac{T_{a,i} - T_{a,o}}{T_{a,i} - T_{wb}} \tag{62}$$

Eq.(55) works well for DEC systems because the cooling process (an adiabatic process) occurs nearly at a constant wet bulb temperature of the inlet air. The wet bulb temperature can be computed using eq.(63)[20].

$$T_{wb} = 2.265 \times \left[1.97 + \left(4.3 \times T_{db,i}\right) + \left(10^4 \times \omega_{a,i}\right)\right]^{\frac{1}{2}} - 14.85 \tag{63}$$

Saturation efficiency of the system: If the exchange surface area is known, then we can calculate the saturation efficiency of the system also known as wet bulb effectiveness.

$$\frac{d\omega_a}{dx} = \frac{A\rho_a h_m}{L\dot{m}_a}(\omega_{vs} - \omega_a) \tag{64}$$

$$\int_{\omega_{a,i}}^{\omega_{a,o}} \frac{-d\omega_a}{\omega_{vs} - \omega_a} = -\int_0^L \frac{A\rho_a h_m}{L\dot{m}_a} dx \tag{65}$$

$$ln\ ln\ \frac{\omega_{vs} - \omega_{a,o}}{\omega_{vs} - \omega_{a,i}} = -\frac{A\rho_a h_m}{\dot{m}_a} \tag{66}$$

$$\frac{\omega_{vs} - \omega_{a,i} + \omega_{a,i} - \omega_{a,o}}{\omega_{vs} - \omega_{a,i}} = 1 - \frac{\omega_{a,o} - \omega_{a,i}}{\omega_{vs} - \omega_{a,i}} = Exp\left[-\frac{A\rho_a h_m}{\dot{m}_a}\right] \tag{67}$$

$$\eta_{sat} = \frac{\omega_{a,o} - \omega_{a,i}}{\omega_{vs} - \omega_{a,i}} = 1 - Exp\left[-\frac{A\rho_a h_m}{\dot{m}_a}\right] \tag{68}$$

This equation shows that high saturation efficiency requires a combination of a large exchange surface area, a high heat/mass transfer coefficient, and a low mass flow rate. The mass flow rate of air is calculated by eq.(69):

$$\dot{m}_a = \rho_a \times A_c \times V_a \tag{69}$$

Outlet air specific and relative humidity:

The humidity ratio of outlet air is deduced from eq.(68).

$$\omega_{a,o} = \omega_{a,i} + \eta_{sat}(\omega_{vs} - \omega_{a,i}) \tag{70}$$

The moisture content of the saturated air (ω_{vs}) is evaluated at the wet bulb temperature using equation (71)[20] :

$$\omega_{vs} = \frac{0.622 \times P_{sat}}{101325 - P_{sat}} \tag{71}$$

Where saturation pressure is calculated by[19], [23]:

$$P_{sat} = 10^5 \times exp\ exp\left\{\left[12.1929 - \frac{4109.1}{(T_{wb} + 273.15) - 35.50}\right]\right\} \tag{72}$$

The relative humidity is computed from the specific humidity of the outlet air using eq.(73)[20]:

$$\emptyset_{a,o} = \frac{100 \times P_{atm}\omega_{a,o}}{P_{sat} \times (0.622 + \omega_{a,o})} \quad (73)$$

Where P_{atm} is the atmospheric pressure and P_{sat} is the saturation pressure evaluated at the outlet air temperature.

Cooling capacity (cc): The cooling capacity is the change in air sensible heat across the air channels of the DEC and is written as:

$$CC = \rho_a.\dot{V}_{a,o}.C_{pa}(T_{a,i} - T_{a,o}) \quad (74)$$

Where ρ_a is the supply air density, and C_{pa} is the specific heat capacity at a constant pressure of the supply air ($J.kg^{-1}.K^{-1}$).

Water evaporation rate (m_e): The humidity of the dry air increases during its passage through the cooling pad due to the mass transfer of water vapor to the air. The following equation gives the amount of water evaporated (rate of water consumption).

$$m_e = \rho_a.\dot{V}_{a,o}.(\omega_{a,o} - \omega_{a,i}) \quad (75)$$

Where $\omega_{a,i}$ and $\omega_{a,o}$ are the humidity ratios at the inlet and the outlet, respectively.

Heat and mass transfer coefficients: Modeling evaporative cooling systems presents a significant challenge in determining precise values for heat and mass transfer coefficients, (h_a) and (h_m). This difficulty arises from the intricate fluid dynamics process through a wet medium, where airflow is governed by continuity, momentum, mass, and energy conservation equations. Consequently, theoretical methods for calculating these transfer coefficients are likely to be inadequate. The most reliable approach remains using correlations based on experimental measurements. To calculate the heat transfer coefficient, the first step is to determine the Reynolds number (Re_a) and the Prandtl number ((Pr_a) whose expressions are given below[24]:

$$Re_a = \frac{\rho_a v_a D_e}{\mu_a} \quad (76)$$

$$Pr_{av} = \frac{\mu_a c_{pa}}{\lambda_a} \quad (77)$$

Where μ_a is the dynamic viscosity of air ($N.s/m^2$), ρ_a is the air density ($kg.m^{-3}$), c_{pa} is the specific heat capacity, λ_a is the heat conductivity ($W.m^{-1}.K^{-1}$), v_a is the air velocity ($m.s^{-1}$).

These dimensionless numbers are essential for estimating heat transfer coefficients in various convection scenarios, as they reflect the fluid's flow characteristics and the relationship between momentum transport and thermal transport capacity. The Reynolds number is used to characterize the flow regime (laminar or turbulent), while the Prandtl number correlates the fluid's viscosity with its thermal conductivity. Together, these numbers are used in empirical correlations to estimate the Nusselt number, which in turn is used to calculate the heat transfer coefficient.

Kays [25] developed a correlation for the Nusselt number to estimate the heat transfer coefficient of air during laminar flow (Re < 2300) inside a duct with a constant wall temperature.

$$Nu_a = 3.66 + \frac{0.104(Re_a Pr_a (D_e/L))}{1 + 0.016(Re_a Pr_a (D_e/L))^{0.8}} \quad (78)$$

Dreyer et al.[26] employed the following equation to determine the heat transfer coefficient within a tube under a turbulent airflow regime.

$$Nu_a = \frac{\left(\frac{f_a}{8}\right)(Re_a - 1000)Pr_a\left(1 + \left(\frac{D_e}{L}\right)^{0.67}\right)}{1 + 12.7\left(\frac{f_a}{8}\right)^{0.5}\left(Pr_a{}^{0.67} - 1\right)} \quad (79)$$

Where the friction factor f_a for smooth tubes was defined by

$$f_a = [1.82log_{10}(Re_a) - 1.64]^{-2} \quad (80)$$

Eq.(79) is valid for the following ranges: $2300 < Re_a < 10^6; 0.5 < Pr_a < 10^4; 0 < D_e/L < 1$

The convective heat transfer coefficient, defined below, can be calculated from the above equations[27].

$$h_a = \frac{Nu_a.\lambda_a}{D_e} \quad (81)$$

In the same way, the mass transfer coefficient (h_m) can be determined from eq.(82):

$$h_m = \frac{Sh_a . D}{D_e} \quad (82)$$

Where Sh_a represents the Sherwood number and D the mass diffusivity coefficient. As, the Nusselt number, the Sherwood number can also be obtained by correlation[28]. However, the introduction of the Lewis factor makes it possible to deduce h_m directly from h_a. Lewis factor (Le_f) different from Lewis number(Le), indicates the relative rate of heat and mass transfer during an evaporation process. Its expression is given below[29]:

$$Le_f = \frac{h_a}{\rho_a c_{pa} h_m} = Le^{\frac{2}{3}} \quad (83)$$

Where Le is known as Lewis number and is defined as:

$$Le = \frac{\alpha}{D} = \frac{Sc_a}{Pr_a} \quad (84)$$

Where α is the heat diffusivity coefficient of air and Sc_a represents the Schmidt number.

Assuming the Lewis factor as unity, which is the same assumption made in previous works [30,31], h_m can be calculated if the air heat capacity ($\rho_a c_{pa}$) and the convective heat transfer coefficient (h_a) are known. This is probably quite accurate for air-water vapor systems with low evaporation rates at atmospheric pressure within simple geometric configurations. Based on this assumption, the mass transfer coefficient is approximated using eq.(85).

$$h_m = \frac{h_a}{\rho_a c_{pa}} \quad (85)$$

Thermophysical properties of air, water, vapor, and air-water vapor mixtures: The presented physical model needs to be connected with psychometric correlation equations that calculate the thermodynamic values of the moist air. The specific heat, density, conductivity, and viscosity of dry air, water vapor, and moist air are computed, using temperature-dependent correlation equations from[21]. They are calculated from the pure component data using mixing rules applicable to any multi-component mixtures [32]. These correlations are derived from theory as well as from numerical fitting procedures and give expressions for density, viscosity, thermal conductivity, and specific heat at the atmospheric pressure and for a temperature range from 220 K to 380 K. Since the process happens at the atmospheric pressure, these psychometric variables used in the model are treated as temperature-dependent. The correlation equations are sufficiently accurate for most engineering calculations in air-conditioning practice and are readily adapted to either hand or computer calculating methods.

Computer calculation procedure: To investigate the performance of the proposed cooling system, an R software programming code is developed based on the above-mentioned equations following a structural approach that involves setting up the simulation environment, defining the physical parameters of the system and the thermodynamic properties of the process air, and applying the relevant equations that describe the cooling process of the system. A preliminary simulation study is performed first to compare the results with experimental data to validate the accuracy of the model. The goal is to examine the evolution of the air temperature and humidity along the wet tube channel for different operating conditions. Fig. 3 shows the flowchart of the computational procedure.

Model validation: Currently, there is no existing research specifically focused on modeling tube-type cross-flow direct evaporative cooling systems, which makes it difficult to directly validate the accuracy of the present tubular heat and mass exchanger model. However, given its similar underlying physics to a plate-type evaporative cooler, the model can be indirectly validated against a plate-type cooler[33]. Using comparable parameters, it is reasonable to expect that this model could apply to plate-type systems as well.

To validate the model, the numerical approach developed by Kovačević et al.[34] for a plate-type evaporative cooler was used as a benchmark. The geometric dimensions of the cooler were aligned with those in the Kovačević model, maintaining consistent values for the hydraulic diameter (3.4 mm) and tube length (9 cm). As illustrated in Fig. 4 the predicted outlet air temperature from the current model closely matches the results from Kovačević et al.'s numerical model when either the inlet air temperature or relative humidity is varied individually, although some deviations were observed at specific inlet conditions. The maximum discrepancy between the two models is less than 4% when the inlet air temperature is below 40.0°C. Additionally, while the root mean

square deviation (RMSD) remains low overall, it tends to increase with higher humidity levels in the intake air.

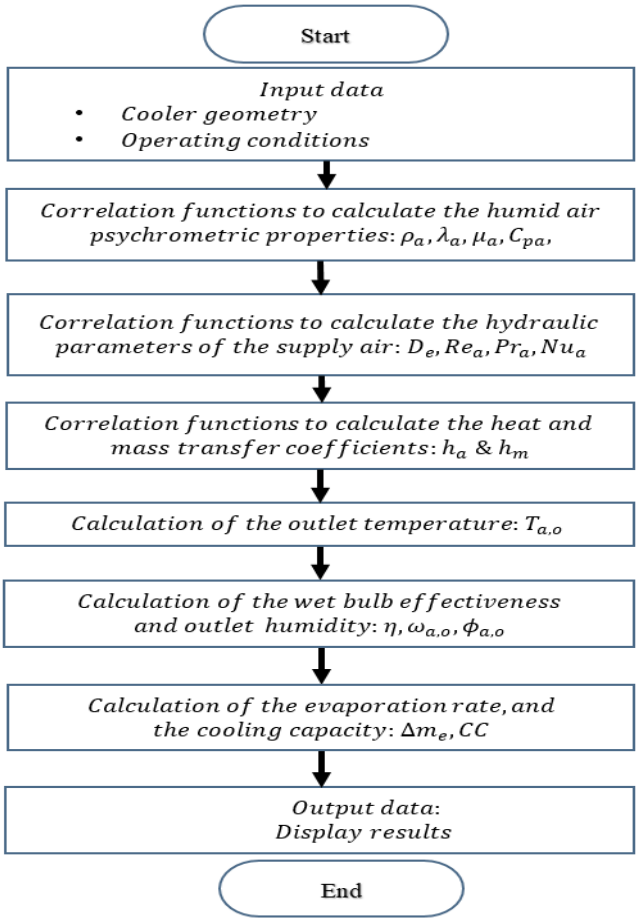

Fig. 3. Flowchart of the computational procedure

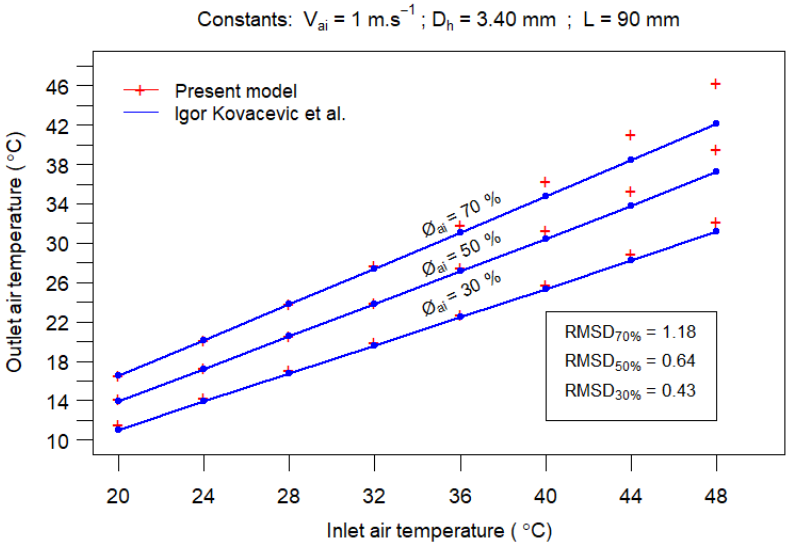

Fig. 4. Validation of our results with the one of Igor Kovačević et al. [34]

3. RESULTS AND DISCUSSION

Understanding the effect of various design parameters on cooling performance is critical for improving the heat and mass transfer characteristics of the exchanger. This section investigates the impact of some structural parameters using the validated model. The parameters under study have been varied while keeping the rest constant. The performance metrics of the study are the air outlet temperature, the sensible cooling capacity, the wet bulb effectiveness, and the water evaporation rate.

3.1 Influence of Tube's Geometrical Parameters on the Outlet Air Temperature

The results depicted in Fig. 5 demonstrate how the outlet temperature of a tubular heat and mass exchanger is affected by the geometrical parameters of the tubes, including equivalent diameter, flatness ratio, and length. Firstly, an increase in the equivalent diameter of the tubes corresponds to a rise in the outlet temperature. This inverse relationship aligns with existing research, which suggests that larger diameters reduce the surface area-to-volume ratio, thereby diminishing heat and mass transfer efficiency[34]. For instance, Sun et al.[35] found that smaller diameters enhance cooling performance due to better contact between the air and the wetted surface. However, they also highlighted the fragility of smaller pipes, leading to a recommended inner diameter of 20 mm for the prototype after considering these factors. Secondly, the flatness ratio, defined as the ratio of the tube's width to its height, also impacts the outlet temperature. As the flatness ratio increases, the outlet temperature decreases. This observation supports studies that highlight the benefits of flat tubular designs. Flat tubes offer a larger surface area for heat and mass transfer compared to round tubes with the same hydraulic diameter. Gao et al.[36] demonstrated that a flat tubular design in a dew-point evaporative cooler improves cooling performance by increasing the surface area, resulting in lower outlet temperatures and better humidity control. Lastly, increasing the tube length leads to a reduction in the outlet temperature. Longer tubes provide more contact time between the air and the wetted surface, thereby enhancing evaporative cooling and heat transfer. However, the graph suggests diminishing returns as the tube length continues to increase. This finding is consistent with studies that emphasize the role of contact time in evaporative cooling. Ramkumar et al.[37] noted that while longer configurations improve performance, there is an optimal length beyond which additional benefits plateau.

3.2 Influence of Tube's Geometrical Parameters on the Cooling Capacity

Fig. 6 indicates that increasing the equivalent diameter results in an increase in cooling capacity, which is consistent with findings in various studies. For example, Li et al. [38] noted that higher hydraulic diameters enhance cooling capacity due to increased heat transfer exchange area. This trend is further supported by the work of Sun et al. [14], who found that higher diameters can significantly improve heat transfer rates in specific applications, such as in compact heat exchangers. However, larger equivalent diameters can cause a transition from laminar to turbulent flow, reducing the Nusselt number and heat transfer rates and causing cooling capacity to decrease drastically. This phenomenon is highlighted in the literature, where turbulent flow is shown to reduce the Nusselt number, adversely affecting heat transfer rates [39]. The impact of the flatness ratio on cooling performance is another critical finding. Increasing the flatness ratio enhances cooling capacity, as flat tubes provide a larger surface area for heat exchange compared to round tubes of the same equivalent diameter. This observation is corroborated by research that emphasizes the advantages of flat tubular designs. For instance, the study by Hasan et al. [16] demonstrated that an oval tubular evaporative cooler outperformed plain tubular evaporative coolers due to its increased surface area, leading to improved cooling metrics. This trend is further supported by the work of Cui et al. [40], who found that flat tube geometry can significantly improve the cooling capacity, while providing superior wetting characteristics, leading to better formation of water films and more efficient use of water's latent heat. Fig. 6 also indicates that longer tubes correlate with higher cooling capacity, indicating improved cooling performance. This is consistent with the literature, which emphasizes the importance of extended contact time between the air and the wetted surface in enhancing evaporative cooling [41]. However, the susceptibility of porous ceramics to damage with longer tubes necessitates a careful balance

between tube length and material durability. This aligns with the insights from sun et al. [35] work, where the trade-offs between system effectiveness and material constraints were discussed.

3.3 Influence of Tube's Geometrical Parameters on the Wet Bulb Effectiveness

Fig. 7 reveals several key findings regarding the impact of geometric parameters on the Wet Bulb Effectiveness. Smaller diameters enhance cooling efficiency by improving contact between the air and wetted surfaces, thus facilitating better heat transfer and therefore the Wet Bulb Effectiveness. However, increasing the tube's equivalent diameter reduces surface area-to-volume ratio which lowers heat and mass transfer efficiency, resulting in decreased wet bulb effectiveness. Moreover, the transition from laminar to turbulent flow at larger diameters exacerbate performance declines. In contrast to the equivalent diameter, higher flatness ratios improve wet bulb effectiveness because flat tubes offer a larger surface area for heat exchange compared to round tubes of the same equivalent diameter. For example, it is observed that increasing the flatness ratio from 1 (circular shape) to 4 greatly expands the surface area-to-volume ratio, resulting in better Wet Bulb Effectiveness. Furthermore, longer tubes enhance cooling performance by lowering outlet temperatures due to extended contact time between the air and the wetted surface, which improves the evaporative cooling effect. Adam et al. [13] observed a similar trend in their study. However, there is an optimal tube length where cooling benefits peak, beyond which further elongation does not provide significant gains. Study by Sun et al. [35] also highlights that longer tubes can make porous ceramics more susceptible to damage, suggesting a need to balance tube length with material durability.

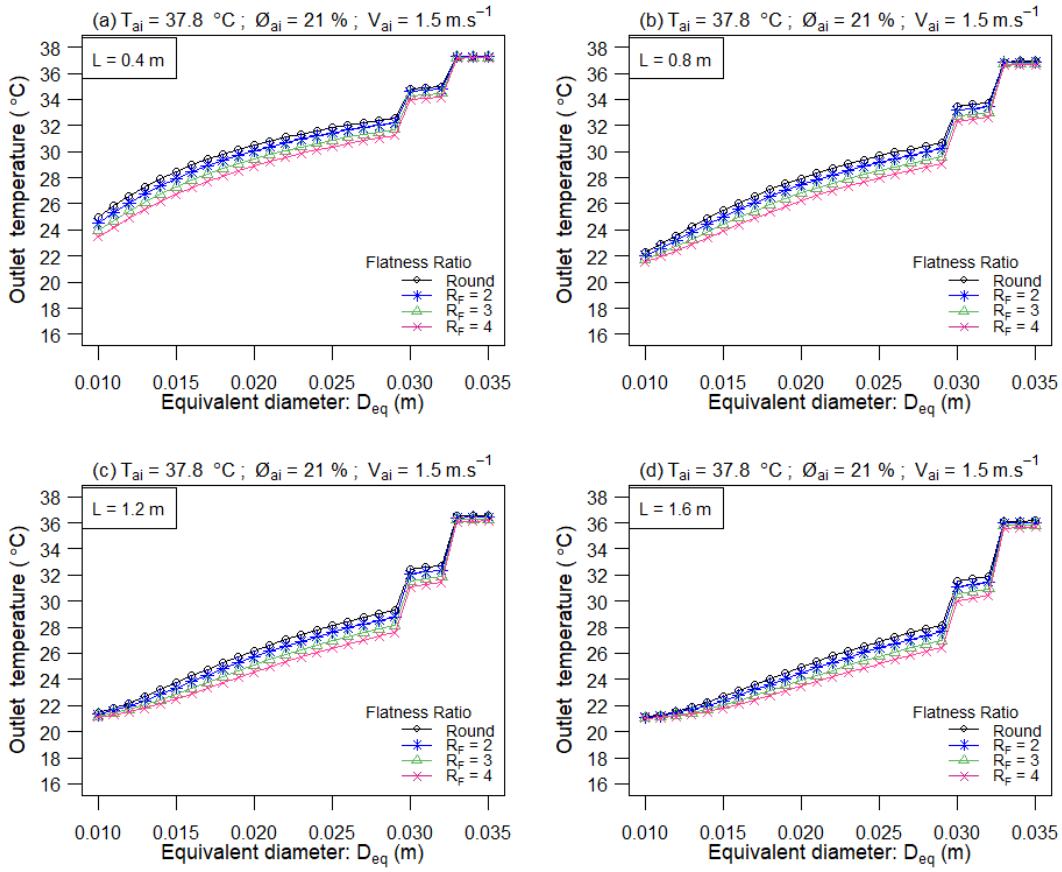

Fig. 5. Influence of tube's geometrical parameters on the outlet air temperature

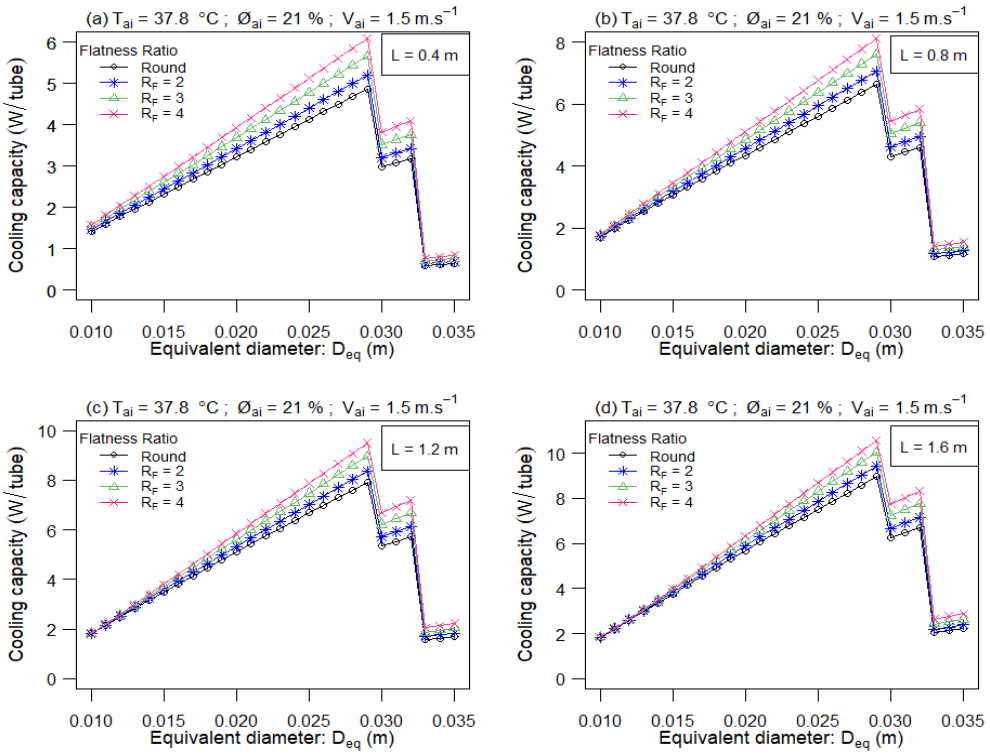

Fig. 6. Influence of tube's geometrical parameters on the cooling capacity

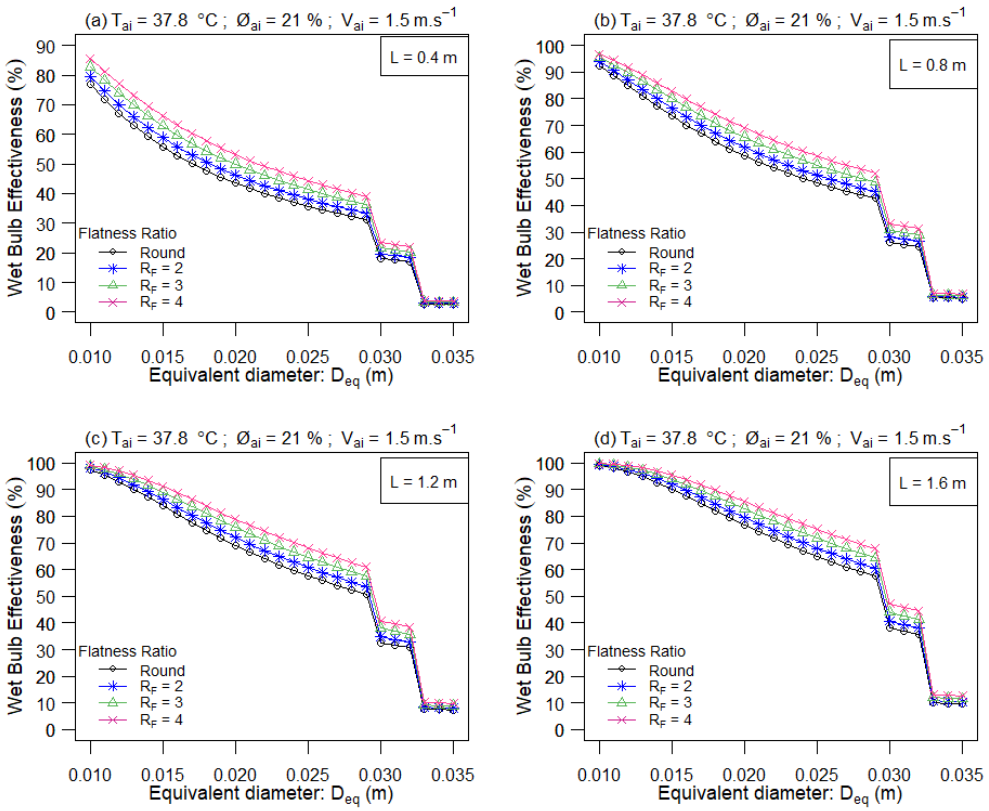

Fig. 7. Influence of tube's geometrical parameters on the wet bulb effectiveness

4. CONCLUSION

This paper presents a study that examines the impact of heat and mass exchanger design parameters on the performance of a terracotta tube-type evaporative cooling system. To achieve this objective, a mathematical model was developed based on the theory of double film and using heat and mass conservation principles. The model was validated against numerical simulation results from existing literature. Simulations were performed under various geometrical parameters to assess their effects on outlet air temperature, cooling capacity, and wet-bulb effectiveness. The key findings from this comprehensive analysis are summarized as follows:

- Increasing the tube equivalent diameter leads to increase in outlet temperature and cooling capacity but decreases the Wet bulb Effectiveness.
- The flatness ratio significantly impacts cooling performance, with increased flatness leading to enhanced cooling capacity and improved wet bulb effectiveness.
- Longer tubes correlate with lower outlet temperatures, enhance Wet Bulb Effectiveness, and higher cooling capacity, indicating improved cooling performance.

This study provides valuable insights for designing and optimizing tubular evaporative cooling systems. It highlights the importance of selecting appropriate tube dimensions to achieve the desired outlet temperature and cooling efficiency. By carefully balancing the hydraulic diameter, flatness ratio, and tube length, engineers can create compact and effective evaporative cooling systems suitable for various applications.

DISCLAIMER (ARTIFICIAL INTELLIGENCE)

Author(s) hereby declare that NO generative AI technologies such as Large Language Models (ChatGPT, COPILOT, etc.) and text-to-image generators have been used during the writing or editing of this manuscript.

ACKNOWLEDGEMENTS

This paper was supported by a Research Grant from the Federal Ministry of Education and Research of Germany through a Graduate Research Program on Climate Change and Energy (GRP-CCE) at the University ABDOU Moumouni de Niamey, Niger. The program is under the control of WASCAL, the West African Science Service Center on Climate Change and Adapted Land Use.

COMPETING INTERESTS

Authors have declared that no competing interests exist.

REFERENCES

1. Romero-Lara MJ, Comino F, de Adana MR. Seasonal energy efficiency ratio of regenerative indirect evaporative coolers—Simplified calculation method. Appl. Therm. Eng. 2023;220:119710.
2. Alawadhi M, Phelan PE. Review of residential air conditioning systems operating under high ambient temperatures. Energies. 2022;15(8):2880.
3. Mousavi S, Gijón-Rivera M, Rivera-Solorio C, Rangel CG. Energy, comfort, and environmental assessment of passive techniques integrated into low-energy residential buildings in semi-arid climate. Energy Build. 2022;263:112053.
4. Sajjad U et al. A review of recent advances in indirect evaporative cooling technology. Int. Commun. Heat Mass Transf. 2021; 122:105140.
5. Li S, Jeong JW. Energy performance of liquid desiccant and evaporative cooling-assisted 100% outdoor air systems under various climatic conditions. Energies. 2018;11(6):1377.
6. Abdullah S et al. Technological development of evaporative cooling systems and its integration with air dehumidification processes: A review. Energy Build. 2023;283:112805.
7. Chen W, Liu S, Lin J. Analysis on the passive evaporative cooling wall constructed of porous ceramic pipes with water sucking ability. Energy Build. 2015; 86:541–549.
8. Wang F, Sun T, Huang X. Experimental research on a novel porous ceramic tube type indirect evaporative cooler. Appl. Therm. Eng. 2017;125:1191–1199.
9. Martınez FR, Gómez EV, Martín RH, Gutiérrez JM, Diez FV. Comparative study of two different evaporative systems: an indirect evaporative cooler and a semi-indirect ceramic evaporative cooler. Energy Build. 2004;36(7):696–708.

10. Gomes E, Martinez FR, Diez FV, Leyva MM. Description and Experimental results of a semi-indirect ceramic evaporative cooler. Int. J. Refrig. 2005;28:654–662.
11. Amer O, Boukhanouf R. Experimental investigation of a novel heat pipe and porous ceramic based indirect evaporative cooler; 2016.
12. Rajski K, Danielewicz J, Brychcy E. Performance evaluation of a Gravity-Assisted heat Pipe-Based indirect evaporative cooler. Energies. 2020;13(1): 200.
13. Adam A, Han D, He W, Amidpour M. Analysis of indirect evaporative cooler performance under various heat and mass exchanger dimensions and flow parameters. Int. J. Heat Mass Transf. 2021;176:121299.
14. Sun T, Tang T, Yang C, Yan W, Cui X, Chu J. Cooling performance and optimization of a tubular indirect evaporative cooler based on response surface methodology. Energy Build. 2023; 285:112880.
15. Sulaiman MA, Adham AM. Evaluation of new dew point evaporative cooler heat and mass exchanger designs with different geometries. Build. Serv. Eng. Res. Technol. 2023;44(4):405–422.
16. Hasan A, Sirén K. Performance investigation of plain circular and oval tube evaporatively cooled heat exchangers. Appl. Therm. Eng. 2004;24(5–6):777–790. DOI:10.1016/j.applthermaleng.2003.10.022.
17. Liu Z, Quan Z, Zhao Y, Jing H, Yang M. Performance optimization of ice thermal storage device based on micro heat pipe arrays. Int. Commun. Heat Mass Transf. 2022;134:106051.
18. Cheng L, Ribatski G, Wojtan L. New flow boiling heat transfer model and flow pattern map for carbon dioxide evaporating inside horizontal tubes. Int. J. Heat Mass Transf. 2006;49(21–22):4082–4094.
19. Ambaum MH. Accurate, simple equation for saturated vapour pressure over water and ice. Q. J. R. Meteorol. Soc. 2020;146(733):4252–4258.
20. Joudi KA, Mehdi SM. Application of indirect evaporative cooling to variable domestic cooling load. Energy Convers. Manag. 2000;41(17):1931–1951.
21. Dreyer AA. Analysis of evaporative coolers and condensers.
22. John R Watt, Brown KB. Evaporative Air Conditioning Handbook, Third ed. UK: Chapmann and Hall; 1997.
23. Musa M. Novel evaporative cooling systems for building applications. PhD Diss Univ. Nottm; 2009.
24. Chinenye N, Manuwa S. Heat transfer coefficient and concept of relaxation time in forced air direct evaporative cooling system; 2015.
25. Kays Wm. Numerical solutions for laminar-flow heat transfer in circular tubes. Trans. Am. Soc. Mech. Eng. 1955;77(8):1265–1272.
26. Dreyer A, Erens P. Heat and mass transfer coefficient and pressure drop correlations for a crossflow evaporative cooler. presented at the Proceedings of the Ninth International Heat Transfer Conference, Hemisphere Publ. Co New York, USA. 1990;233–238.
27. Heidarinejad G, Moshari S. Novel modeling of an indirect evaporative cooling system with cross-flow configuration. Energy Build. 2015;92:351–362.
28. Aramayo-Prudencio A, Young J. The Analysis and Design of Saturators for Power Generation Cycles: Part 2—Heat and Mass Transfer. presented at the Turbo Expo: Power for Land, Sea, and Air. 2003;423–432.
29. Kloppers JC, Kröger DG. The Lewis factor and its influence on the performance prediction of wet-cooling towers. Int. J. Therm. Sci. 2005;44(9):879–884.
30. Dai Y, Sumathy K. Theoretical study on a cross-flow direct evaporative cooler using honeycomb paper as packing material. Appl. Therm. Eng. 2002;22(13):1417–1430.
31. Wu J, Huang X, Zhang H. Numerical investigation on the heat and mass transfer in a direct evaporative cooler. Appl. Therm. Eng. 2009;29(1):195–201.
32. Reid R. The Properties of Gases and Liquids; 1987.
33. JIA X. Fundamental design and study of an evaporative cooling system; 2014.
34. Kovačević I, Sourbron M. The numerical model for direct evaporative cooler. Appl. Therm. Eng. 2017;113:8–19.
35. Sun T, Huang X, Qu Y, Wang F, Chen Y. Theoretical and experimental study on heat and mass transfer of a porous ceramic tube type indirect evaporative cooler. Appl. Therm. Eng. 2020;173: 115211.

36. Gao F, Thu K, Wang S. Numerical investigation of a novel tubular dew-point evaporative cooler. Appl. Therm. Eng. 2023;223:120064.
37. Ramkumar R. Experimental investigation of indirect evaporative cooler using clay pipe. J. Therm. Eng. 2017;3(2)1163–1180.
38. Li R, Zhou W, Wu J. Numerical method and analysis of a tube indirect evaporative cooler. Therm. Sci. 2022;26(1 Part A):375–387.
39. Kang M, Elbel S. Comprehensive study of heat transfer and pressure drop in regenerator and optimization of solid-state caloric cooling cycles using realistic hydraulic diameter of regenerator; 2021.
40. Cui X, Zhang Y, Yan W, Yang C, Liu Y, Chua KJ. Statistical modeling and multi-objective optimization of a flat tubular indirect evaporative cooler for enhanced performance. Appl. Therm. Eng. 2024; 123538.
41. Sellami K, Feddaoui M, Labsi N, Najim M, Oubella M, Benkahla YK. Direct evaporative cooling performance of ambient air using a ceramic wet porous layer. Chem. Eng. Res. Des. 2019;142: 225–236.
DOI: 10.1016/j.cherd.2018.12.009.

Peer-review history:
The peer review history for this paper can be accessed here:
https://www.sdiarticle5.com/review-history/123693